

# An Overloaded SC-CP IoT Signal Detection Method via Sparse Complex Discrete-Valued Vector Reconstruction

Kazunori Hayashi\*, Ayano Nakai-Kasai†, Ryo Hayakawa†

\* Osaka City University, Osaka, Japan

RIKEN Center for Advanced Intelligence Project

E-mail: kazunori@eng.osaka-cu.ac.jp

† Kyoto University, Kyoto, Japan

E-mail: nakai.ayano@sys.i.kyoto-u.ac.jp, rhayakawa@sys.i.kyoto-u.ac.jp

**Abstract**—The paper proposes low-latency signal detection methods for overloaded MU-MIMO (Multi-User Multi-Input Multi-Output) SC-CP (Single Carrier block transmission with Cyclic Prefix) using convex optimization approach for uplink IoT (Internet of Things) environments where a lot of IoT terminals are served by a base station having less number of antennas than that of IoT terminals. The proposed method detects overloaded IoT signals via convex optimization approach named sum of complex sparse regularizers (SCSR) taking advantage of both the discreteness and the sparsity of the SC-CP IoT signal. Simulation results demonstrate the validity of the proposed method.

## I. INTRODUCTION

Typical IoT data collection environment using a base station with a large number of antennas in the 5th generation mobile communications systems (5G) [1],[2] can be considered as a massive multi-user multi-input multi-output (MU-MIMO) communications system by regarding each IoT terminal as a transmit antenna. One of fundamental differences between the conventional massive MU-MIMO [3],[4] and the IoT data collection is that the number of IoT nodes, in other words, the number of transmit antennas is typically much greater than that of receiving antennas even when a large antenna array is employed at the base station. Combined use with multiple access schemes will enable us to serve a large number of IoT nodes, but it also introduces additional delay, which may not be acceptable in many IoT applications.

MIMO systems having greater number of transmit antennas (transmit streams) than that of receiving antennas is called overloaded MIMO. The signal detection problem in such scenario is very difficult due to the underdetermined nature of the problem, however, if the transmit symbol takes discrete values on a finite set as in the case of digital communications, we can detect signals based on maximum likelihood (ML) approach[5]. In the case of massive overloaded MIMO detection, since the ML approach is not tractable, we have

proposed a signal detection scheme using SOAV (Sum-of-Absolute-Values) optimization[8], which is based on the idea of convex optimization and compressed sensing[6], [7]. This approach is especially effective when the number of antennas is large and the number of elements in the alphabet is small.

Taking advantage of the fact that the transmission rate from each IoT node is typically low, we have proposed a detection scheme for uplink OFDM (Orthogonal Frequency Devision Multiplexing) IoT signals[9], where the overloaded MIMO signal reconstruction scheme in [8] is employed. In [9], it has been shown that the proposed IoT signal detection can achieve almost the same performance as in the case with the i.i.d. Gaussian measurement matrix, which can be considered as an ideal case, by multiplying a common Hadamard matrix at IoT nodes (transmitters) as a precoding matrix. However, the proposed method cannot take the dependency between the real and the imaginary parts of the transmitted symbol into consideration, since it has utilized the SOAV optimization in real domain, and thus it sometimes returns the reconstruction result of  $1+0j$  even when the alphabet of transmitted symbol is  $\{0, 1+j, -1+j, 1-j, -1-j\}$ , where 0 means non-active terminal. Namely, the method in [9] cannot use the fact that the real and the imaginary parts becomes 0 simultaneously.

In this paper, we consider the overloaded MU-MIMO SC-CP (Single Carrier block transmission with Cyclic Prefix) without precoding because it is equivalent to the MU-MIMO OFDM with precoding by a common discrete Fourier transform (DFT) matrix, while neither the operations of inverse DFT nor the precoding is not required at the transmitter, which can greatly reduce the complexity of IoT nodes. Moreover, we employ a sparse complex discrete-valued vector reconstruction scheme named sum of complex sparse regularizers (SCSR) optimization in [10], in order to appropriately treat the symbol of 0 by non-active terminals. Validity of the proposed approach is confirmed via computer simulations compared to the performance of the signal reconstruction method in [9].

In the rest of the paper, we use the following notations.  $\mathbb{R}$  is the set of all real numbers and  $\mathbb{C}$  is the set of all complex numbers. We represent the transpose by  $(\cdot)^T$ , the Hermitian

---

This work was partially supported by the R&D contract (FY2017–2020) “Wired-and-Wireless Converged Radio Access Network for Massive IoT Traffic” for radio resource enhancement by the Ministry of Internal Affairs and Communications, Japan.

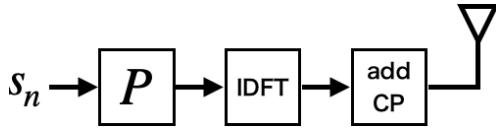


Fig. 1. Transmitter structure of precoded OFDM

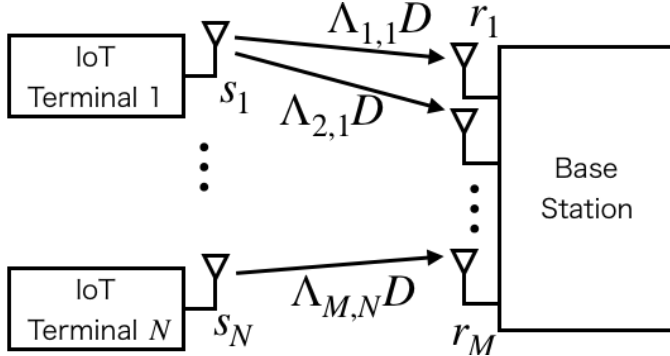


Fig. 2. Uplink of IoT environment using SC-CP signaling

transpose by  $(\cdot)^H$ , the imaginary unit by  $j$ , the  $N \times N$  identity matrix by  $\mathbf{I}_N$ , a vector of size  $N \times 1$  whose elements are all 1 by  $\mathbf{1}_N$ , and a vector of size  $N \times 1$  whose elements are all 0 by  $\mathbf{0}_N$ .  $\text{Re}\{\cdot\}$  and  $\text{Im}\{\cdot\}$  denote the real part and the imaginary part, respectively. For  $\mathbf{u} = [u_1 \cdots u_N]$  and some operator  $f$ ,  $[f(\mathbf{u})]_n$  and  $u_n$  denote the  $n$ -th element of  $f(\mathbf{u})$  and  $\mathbf{u}$ , respectively.

## II. SYSTEM MODEL

Here, we firstly show that MU-MIMO SC-CP signal can be regarded as a special case of the precoded MU-MIMO OFDM, where the DFT matrix is employed as the precoding matrix.

The frequency domain received signal model of precoded MU-MIMO OFDM in Fig. 1 can be written as [9]

$$\begin{bmatrix} \mathbf{r}_1^{\text{f,ofdm}} \\ \vdots \\ \mathbf{r}_M^{\text{f,ofdm}} \end{bmatrix} = \begin{bmatrix} \Lambda_{1,1}\mathbf{P} & \cdots & \Lambda_{1,N}\mathbf{P} \\ \vdots & & \vdots \\ \Lambda_{M,1}\mathbf{P} & \cdots & \Lambda_{M,N}\mathbf{P} \end{bmatrix} \begin{bmatrix} \mathbf{s}_1 \\ \vdots \\ \mathbf{s}_N \end{bmatrix} + \begin{bmatrix} \mathbf{v}_1^{\text{f}} \\ \vdots \\ \mathbf{v}_M^{\text{f}} \end{bmatrix}, \quad (1)$$

where  $\mathbf{r}_m^{\text{f,ofdm}} \in \mathbb{C}^Q$  ( $m = 1, \dots, M$ ) is the frequency domain received signal block at the  $m$ -th antenna at the base station,  $\mathbf{s}_n$  ( $n = 1, \dots, N$ ) is the transmitted signal block in the frequency domain from the  $n$ -th IoT terminal. Here, taking IoT environment specific feature into consideration, we assume only  $N_o$  IoT terminals out of  $N$  terminals are active and transmit the signal block. Non-active  $N - N_o$  terminals actually keep silent, but we can regard they transmit all zero signal block  $\mathbf{0}_Q$ .  $\mathbf{P} \in \mathbb{C}^{Q \times Q}$  is a precoding matrix required to achieve good detection performance by the convex optimization based detection scheme. Note that, in [9], we have numerically confirmed that we don't have to use different precoding matrices among IoT terminals, and a common Hadamard precoding matrix leads to good symbol error rate (SER) performance.  $\mathbf{v}_m^{\text{f}} \in \mathbb{C}^Q$  is the frequency domain

additive white noise vector at the  $m$ -th receiving antenna having mean  $\mathbf{0}_Q$  and covariance matrix  $\sigma_n^2 \mathbf{I}_Q$ . The frequency domain diagonal channel matrix  $\Lambda_{m,n} \in \mathbb{C}^{Q \times Q}$  between the  $n$ -th IoT terminal and the  $m$ -th receiving antenna is given by using the impulse response of the frequency selective channel  $\{h_1^{(m,n)}, \dots, h_L^{(m,n)}\}$  with the channel order of  $L - 1$  as

$$\begin{bmatrix} \lambda_1^{(m,n)} \\ \vdots \\ \lambda_Q^{(m,n)} \end{bmatrix} = \sqrt{Q} \mathbf{D} \begin{bmatrix} h_1^{(m,n)} \\ \vdots \\ h_L^{(m,n)} \\ \mathbf{0}_{Q-L} \end{bmatrix}, \quad (2)$$

where  $\{\lambda_1^{(m,n)}, \dots, \lambda_Q^{(m,n)}\}$  are diagonal elements of  $\Lambda_{m,n}$  and  $\mathbf{D}$  is a  $Q$ -point DFT matrix defined as

$$\mathbf{D} = \frac{1}{\sqrt{Q}} \begin{bmatrix} 1 & 1 & \cdots & 1 \\ 1 & e^{-j\frac{2\pi \times 1 \times 1}{Q}} & \cdots & e^{-j\frac{2\pi \times 1 \times (Q-1)}{Q}} \\ \vdots & \vdots & \ddots & \vdots \\ 1 & e^{-j\frac{2\pi \times (Q-1) \times 1}{Q}} & \cdots & e^{-j\frac{2\pi \times (Q-1) \times (Q-1)}{Q}} \end{bmatrix}.$$

We then consider the received signal model of SC-CP signaling without precoding. Assuming the length cyclic prefix  $K$  is greater than or equal to the channel order  $L - 1$ , the time domain received signal block at the  $m$ -th receive antenna of the base station is written as

$$\mathbf{r}_m^{\text{t,sccp}} = \mathbf{R}_{\text{cp}} \mathbf{H}_0^{(m,n)} \mathbf{T}_{\text{cp}} \mathbf{s}_n + \mathbf{v}_m^{\text{t}}, \quad (3)$$

where  $\mathbf{v}_m^{\text{t}} \in \mathbb{C}^Q$  is the time domain additive white noise vector at the  $m$ -th receiving antenna having mean  $\mathbf{0}_Q$  and covariance matrix  $\sigma_n^2 \mathbf{I}_Q$ .  $\mathbf{H}_0^{(m,n)}$  is a time domain channel matrix between the  $n$ -th IoT terminal and the  $m$ -th base station antenna given by

$$\mathbf{H}_0^{(m,n)} = \begin{bmatrix} h_1^{(m,n)} & 0 & 0 & \cdots & \cdots & 0 \\ \vdots & h_1^{(m,n)} & \ddots & \ddots & & \vdots \\ h_L^{(m,n)} & & \ddots & & \ddots & \vdots \\ 0 & \ddots & & \ddots & \ddots & \vdots \\ \vdots & & \ddots & & \ddots & 0 \\ 0 & \cdots & 0 & h_L^{(m,n)} & \cdots & h_1^{(m,n)} \end{bmatrix}.$$

Also,  $\mathbf{T}_{\text{cp}}$  is a cyclic prefix insertion matrix defined as

$$\mathbf{T}_{\text{cp}} = \begin{bmatrix} \mathbf{O}_{K \times (Q-K)} & \mathbf{I}_K \\ & \mathbf{I}_Q \end{bmatrix}, \quad (4)$$

and  $\mathbf{R}_{\text{cp}}$  is a cyclic prefix removal matrix given by

$$\mathbf{R}_{\text{cp}} = [\mathbf{0}_{Q \times K} \quad \mathbf{I}_Q]. \quad (5)$$

Then, the overall channel matrix including the impact of cyclic prefix operations as well as the actual frequency selective fading channel  $\mathbf{R}_{\text{cp}} \mathbf{H}_0^{(m,n)} \mathbf{T}_{\text{cp}}$  has a following circulant

structure:

$$\mathbf{R}_{\text{cp}} \mathbf{H}_0^{(m,n)} \mathbf{T}_{\text{cp}} = \begin{bmatrix} h_1^{(m,n)} & 0 & \cdots & 0 & h_L^{(m,n)} & \cdots & h_2^{(m,n)} \\ \vdots & h_1^{(m,n)} & \ddots & & \ddots & \ddots & \vdots \\ h_L^{(m,n)} & & \ddots & \ddots & & \ddots & h_L^{(m,n)} \\ 0 & \ddots & & \ddots & \ddots & & 0 \\ \vdots & \ddots & \ddots & & \ddots & \ddots & \vdots \\ \vdots & & \ddots & \ddots & & \ddots & 0 \\ 0 & \cdots & 0 & h_L^{(m,n)} & \cdots & h_1^{(m,n)} \end{bmatrix}.$$

Since unitary similarity transformation of any circulant matrix is given by DFT matrix, the overall channel matrix can be written as

$$\mathbf{R}_{\text{cp}} \mathbf{H}_0^{(m,n)} \mathbf{T}_{\text{cp}} = \mathbf{D}^H \mathbf{\Lambda}_{m,n} \mathbf{D}, \quad (6)$$

$\mathbf{\Lambda}_{m,n}$  is the same matrix as in (1), whose diagonal elements are defined in (2).

By stacking from  $\mathbf{r}_1^{\text{t,sccp}}$  to  $\mathbf{r}_M^{\text{t,sccp}}$  in (3), and multiplying a unitary matrix

$$\begin{bmatrix} \mathbf{D} & 0 & \cdots & 0 \\ 0 & \mathbf{D} & & \vdots \\ \vdots & & \ddots & 0 \\ 0 & \cdots & \cdots & \mathbf{D} \end{bmatrix} \in \mathbb{C}^{QM \times QM} \quad (7)$$

from the left of both sides, we have the frequency domain received SC-CP IoT signal vector at the base station depicted in Fig. 2 as

$$\begin{aligned} \begin{bmatrix} \mathbf{r}_1^{\text{f,sccp}} \\ \vdots \\ \mathbf{r}_M^{\text{f,sccp}} \end{bmatrix} &= \begin{bmatrix} \mathbf{D} & 0 & \cdots & 0 \\ 0 & \mathbf{D} & & \vdots \\ \vdots & & \ddots & 0 \\ 0 & \cdots & \cdots & \mathbf{D} \end{bmatrix} \begin{bmatrix} \mathbf{r}_1^{\text{t,sccp}} \\ \vdots \\ \mathbf{r}_M^{\text{t,sccp}} \end{bmatrix} \\ &= \begin{bmatrix} \mathbf{\Lambda}_{1,1} \mathbf{D} & \cdots & \mathbf{\Lambda}_{1,N} \mathbf{D} \\ \vdots & & \vdots \\ \mathbf{\Lambda}_{M,1} \mathbf{D} & \cdots & \mathbf{\Lambda}_{M,N} \mathbf{D} \end{bmatrix} \begin{bmatrix} \mathbf{s}_1 \\ \vdots \\ \mathbf{s}_N \end{bmatrix} + \begin{bmatrix} \mathbf{v}_1^{\text{f}} \\ \vdots \\ \mathbf{v}_M^{\text{f}} \end{bmatrix}, \end{aligned} \quad (8)$$

where  $\mathbf{r}_m^{\text{f,sccp}} \in \mathbb{C}^Q$  ( $m = 1, \dots, M$ ) is the frequency domain received SC-CP signal vector at the  $m$ -th base station antenna. It should be noted here that this received signal model can be regarded as a special case of (1), where the precoding matrix  $\mathbf{P}$  is set to be  $\mathbf{D}$ . Thus, if DFT matrix  $\mathbf{D}$  is appropriate for the precoding matrix of overloaded MU-MIMO OFDM system with the convex optimization based signal detection, then the choice of SC-CP signaling is extremely suited for IoT environments because this approach requires neither the IDFT operation nor the precoding operation at the IoT node (transmitter side).

### III. COMPLEX DISCRETE VALUED SIGNAL RECONSTRUCTION VIA SCSR OPTIMIZATION

One of features of the proposed approach in this paper is the employment of SCSR optimization instead of SOAV optimization in [9], which considerably improves the SER performance for IoT environments, where only a subset of IoT nodes are active at a time. Here, we briefly review the complex discrete signal reconstruction via SCSR optimization[10].

Consider the reconstruction problem of a complex discrete-valued vector  $\mathbf{x} = [x_1 \cdots x_N]^H \in \mathcal{C} \subset \mathbb{C}^N$  from a linear measurement of

$$\mathbf{y} = \mathbf{A} \mathbf{x} + \mathbf{v} \in \mathbb{C}^M. \quad (9)$$

Here,  $\mathcal{C} = \{c_1 \cdots c_S\}$  is a set of discrete values, that each element of unknown vector  $\mathbf{x}$  takes, and the probability distribution of each element of  $\mathbf{x}$  is given by

$$\Pr(x_n = c_\ell) = p_\ell, \quad (\ell = 1, \dots, S), \quad (10)$$

$$\sum_{\ell=1}^S p_\ell = 1. \quad (11)$$

$\mathbf{A} \in \mathbb{C}^{M \times N}$  is a measurement matrix and  $\mathbf{v} \in \mathbb{C}^M$  is an additive noise vector with mean of  $\mathbf{0}_M$  and covariance matrix of  $\sigma_v^2 \mathbf{I}_M$ .

The optimization problem for the complex discrete-valued signal reconstruction named SCSR, which is an extension of SOAV optimization for real discrete-valued signal reconstruction, is given by

$$\underset{\hat{\mathbf{x}} \in \mathbb{C}^N}{\text{minimize}} \sum_{\ell=1}^S q_\ell g_\ell(\hat{\mathbf{x}} - c_\ell \mathbf{1}) + \lambda \|\mathbf{y} - \mathbf{A} \hat{\mathbf{x}}\|_2^2, \quad (12)$$

where  $\lambda \geq 0$  and  $q_\ell \geq 0$  ( $\ell = 1, \dots, S$ ) are parameters.  $g_\ell(\cdot)$  is a function for the sparse regularizer, and in this paper, we consider two possible options for the function as

$$h_1(\mathbf{u}) = \|\mathbf{u}\|_1 = \sum_{n=1}^N \sqrt{\text{Re}\{u_n\}^2 + \text{Im}\{u_n\}^2}, \quad (13)$$

$$h_2(\mathbf{u}) = \|\text{Re}\{\mathbf{u}\}\|_1 + \|\text{Im}\{\mathbf{u}\}\|_1 \quad (14)$$

$$= \sum_{n=1}^N (|\text{Re}\{u_n\}| + |\text{Im}\{u_n\}|). \quad (15)$$

SCSR optimization problem (12) can be solved by ADMM (Alternating Direction Method of Multipliers) based computationally efficient algorithm (Algorithm 1). The proximity operators of  $\gamma h_1(\cdot)$ ,  $\gamma h_2(\cdot)$  ( $\gamma > 0$ ) required in the algorithm are given by

$$[\text{prox}_{\gamma h_1}(\mathbf{u})]_n = \begin{cases} (|u_n| - \gamma) \frac{u_n}{|u_n|} & (|u_n| \geq \gamma) \\ 0 & (|u_n| < \gamma), \end{cases}$$

$$[\text{prox}_{\gamma h_2}(\mathbf{u})]_n = \text{sign}([\text{Re}(\mathbf{u})]_n) \max(|[\text{Re}(\mathbf{u})]_n| - \gamma, 0) + j \cdot \text{sign}([\text{Im}(\mathbf{u})]_n) \max(|[\text{Im}(\mathbf{u})]_n| - \gamma, 0),$$

where  $\mathbf{u} = [u_1 \cdots u_N] \in \mathbb{C}^N$ .

---

**Algorithm 1** SCSR
 

---

**Require:**  $\mathbf{y} \in \mathbb{C}^M, \mathbf{A} \in \mathbb{C}^{M \times N}$ 
**Ensure:**  $\hat{\mathbf{x}} \in \mathbb{C}^N$ 

- 1: Fix  $\rho > 0, \mathbf{z}^0 \in \mathbb{C}^{SN}, \mathbf{w}^0 \in \mathbb{C}^{SN}$
  - 2: **for**  $k = 0$  to  $K - 1$  **do**
  - 3:  $\mathbf{s}^{k+1} = (\rho S \mathbf{I}_N + \lambda \mathbf{A}^H \mathbf{A})^{-1} (\rho \sum_{\ell=1}^S (\mathbf{z}_\ell^k - \mathbf{w}_\ell^k) + \lambda \mathbf{A}^H \mathbf{y})$
  - 4:  $\mathbf{z}_\ell^{k+1} = c_\ell \mathbf{1} + \text{prox}_{\frac{q_\ell}{2\rho} g_\ell}(\mathbf{s}^{k+1} + \mathbf{w}_\ell^k - c_\ell \mathbf{1}) \quad (\ell = 1, \dots, S)$
  - 5:  $\mathbf{w}_\ell^{k+1} = \mathbf{w}_\ell^k + \mathbf{s}^{k+1} - \mathbf{z}_\ell^{k+1} \quad (\ell = 1, \dots, S)$
  - 6: **end for**
  - 7:  $\hat{\mathbf{x}} = \mathbf{s}^K$
- 

If we define the function of sparse regularizer  $g_\ell(\cdot)$  to be an element wise function, we can extend the SCSR optimization (12) to a weighted SCSR optimization problem of

$$\underset{\mathbf{x} \in \mathbb{C}^N}{\text{minimize}} \sum_{\ell=1}^S \sum_{n=1}^N q_{n,\ell} g_\ell(x_n - c_\ell) + \lambda \|\mathbf{y} - \mathbf{A}\mathbf{x}\|_2^2, \quad (16)$$

where different weight  $q_{n,\ell}$  can be set for each element  $x_n$ . Moreover,  $q_{n,\ell}$  can be updated iteratively by using the estimate obtained in the previous iteration round. Specifically, we employ following update equation [10] for the parameter update

$$q_{n,\ell} = \frac{|\hat{x}_n^{\text{pre}} - c_\ell|^{-1}}{\sum_{\ell'=1}^S |\hat{x}_n^{\text{pre}} - c_{\ell'}|^{-1}}, \quad (17)$$

where  $\hat{x}_n^{\text{pre}}$  is the  $n$ -th element of the estimate in the previous iteration round. Also, for some fixed parameter  $\beta$ , the parameter  $\lambda$  in (16) is set to be

$$\frac{\mathbb{E}[\sum_{\ell=1}^S \sum_{n=1}^N q_{n,\ell} g_\ell(x_n - c_\ell)]}{\mathbb{E}[\lambda \|\mathbf{y} - \mathbf{A}\mathbf{s}\|_2^2]} = \beta, \quad (18)$$

in order to adaptively adjust the balance between the regularization term and the data fidelity term.

The algorithm to solve the iterative weighted SCSR (IW-SCSR) optimization problem also can be derived by the ADMM framework, which is shown in Algorithm 2.

#### IV. SC-CP IoT SIGNAL DETECTION VIA IW-SCSR

A generalized form of the time domain received signal vector  $\mathbf{r} \in \mathbb{C}^{QM}$  in (8) can be given by

$$\mathbf{r} = \mathbf{H}\mathbf{s} + \mathbf{v}, \quad (19)$$

where  $\mathbf{s} \in \mathbb{C}^{QN}$  is a transmitted signal vector,  $\mathbf{H} \in \mathbb{C}^{QM \times QN}$  is a channel matrix, and  $\mathbf{v} \in \mathbb{C}^{QM}$  is a white noise vector. The weighted SCSR optimization problem for (19) is given by

$$\underset{\mathbf{s} \in \mathbb{C}^{QN}}{\text{minimize}} \sum_{\ell=1}^S \sum_{n=1}^N q_{n,\ell} g_\ell(s_n - c_\ell) + \lambda \|\mathbf{r} - \mathbf{H}\mathbf{s}\|_2^2. \quad (20)$$

If we assume QPSK modulation, we have  $S = 5, (c_1, c_2, c_3, c_4, c_5) = \{0, 1 + j, -1 + j, 1 - j, -1 - j\}$ . Note that, if transmit symbol does not include non-active

---

**Algorithm 2** IW-SCSR
 

---

**Require:**  $\mathbf{y} \in \mathbb{C}^M, \mathbf{A} \in \mathbb{C}^{M \times N}$ 
**Ensure:**  $\hat{\mathbf{x}} \in \mathbb{C}^N$ 

- 1: Initialize  $q_{n,\ell} (n = 1, \dots, N \text{ and } \ell = 1, \dots, S)$
  - 2: **for**  $t = 1$  to  $T$  **do**
  - 3: Fix  $\beta > 0, \rho > 0, \mathbf{z}^0 \in \mathbb{C}^{SN}, \mathbf{w}^0 \in \mathbb{C}^{SN}$
  - 4:  $\lambda = \frac{\sum_{\ell'=1}^S p_{\ell'} \sum_{\ell=1}^S \sum_{n=1}^N q_{n,\ell} g_\ell(c_{\ell'} - c_\ell)}{\beta M \sigma^2}$
  - 5: **for**  $k = 0$  to  $K - 1$  **do**
  - 6:  $\mathbf{s}^{k+1} = (\rho S \mathbf{I}_N + \lambda \mathbf{A}^H \mathbf{A})^{-1} (\rho \sum_{\ell=1}^S (\mathbf{z}_\ell^k - \mathbf{w}_\ell^k) + \lambda \mathbf{A}^H \mathbf{y})$
  - 7:  $\mathbf{z}_{n,\ell}^{k+1} = c_\ell + \text{prox}_{\frac{q_{n,\ell}}{2\rho} g_\ell}(\mathbf{s}_n^{k+1} + \mathbf{w}_{n,\ell}^k - c_\ell)$
  - 8:  $(n = 1, \dots, N \text{ and } \ell = 1, \dots, S)$
  - 9:  $\mathbf{w}_\ell^{k+1} = \mathbf{w}_\ell^k + \mathbf{s}^{k+1} - \mathbf{z}_\ell^{k+1} \quad (\ell = 1, \dots, S)$
  - 10: **end for**
  - 11:  $d_{n,\ell} = |s_n^K - c_\ell| \quad (n = 1, \dots, N \text{ and } \ell = 1, \dots, S)$
  - 12:  $q_{n,\ell} = \frac{d_{n,\ell}^{-1}}{\sum_{\ell'=1}^S d_{n,\ell'}^{-1}} \quad (n = 1, \dots, N \text{ and } \ell = 1, \dots, S)$
  - 13: **end for**
  - 14:  $\hat{\mathbf{x}} = \mathbf{s}^K$
- 

IoT terminal (or symbol of 0), the sparse regularizer of  $h_2(\cdot)$  is appropriate for  $g_\ell(\cdot)$ , which is equivalent to the approach using SOAV optimization for real and imaginary parts independently. However, as we'll see in the next section, if we have certain number of non-active terminals, the employment of the sparse regularizer of  $g_1(\cdot) = h_1(\cdot)$  can improve the performance because it can utilize the fact that the real and the imaginary parts of  $c_1$  take the value of 0 simultaneously. After all, we employ

$$g_1(\mathbf{u}) = h_1(\mathbf{u}), \quad (21)$$

$$g_\ell(\mathbf{u}) = h_2(\mathbf{u}) \quad (\ell = 2, \dots, S), \quad (22)$$

for the regularizers.

#### V. NUMERICAL RESULTS

We have conducted numerical experiments via computer simulations to evaluate the SER performance of the proposed overloaded SC-CP signal detection scheme using the frequency domain received signal. The block size of the SC-CP transmission is set to  $Q = 64$ , and the length of the cyclic prefix is assumed to be greater than or equal to the channel order. In order to evaluate the performance of different system size, we have set the number of antennas at the base station  $M$  and the number of IoT terminals  $N$  to be  $(M, N) = (6, 8)$  and  $(M, N) = (60, 80)$ , which correspond to the overloaded factor of about 1.33. We regard non-active terminals transmit symbols of 0, and the number of active terminals  $N_o$  is set so that the ratio of zero symbols over total symbols  $\frac{N - N_o}{N}$  becomes 0.125 or 0.875. The parameters for IW-SCSR algorithm are set to  $\beta = 10, \rho = 0.1$ , and the number of iterations  $T$  of the outer loop of IW-SCSR is 1 or 5. Note that no precoding is employed in the simulations.

As for the reference scheme to compare the performance, we have employed DFISTA (Discreteness-aware FISTA)[8],

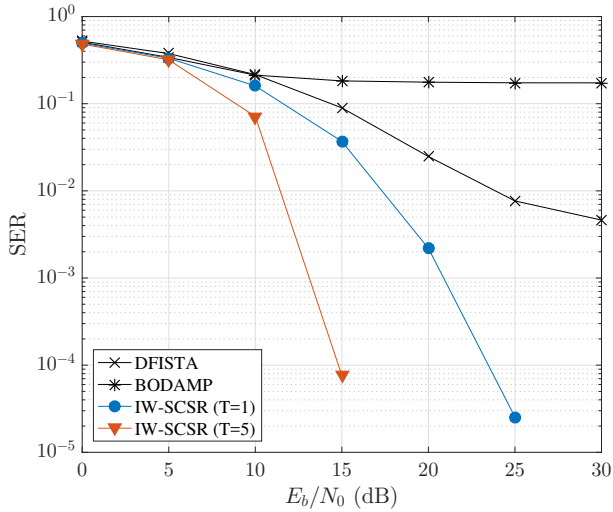


Fig. 3. SER performance ( $M = 6, N = 8, N_o = 7$ )

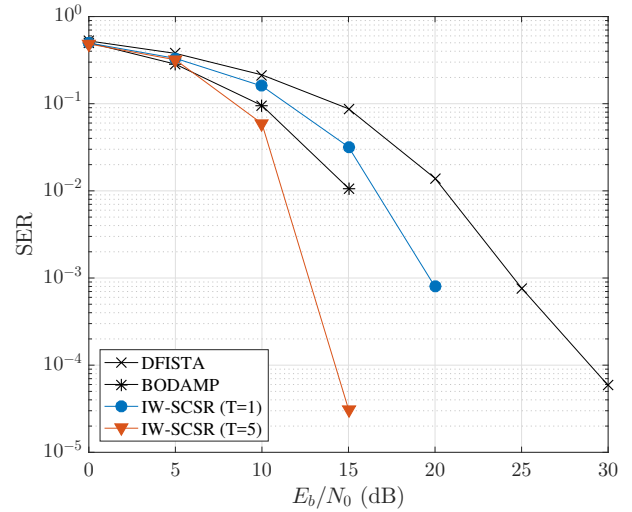


Fig. 5. SER performance ( $M = 60, N = 80, N_o = 70$ )

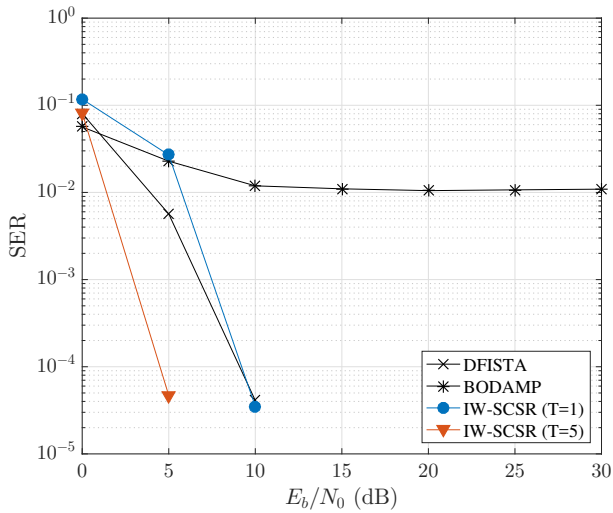


Fig. 4. SER performance ( $M = 6, N = 8, N_o = 1$ )

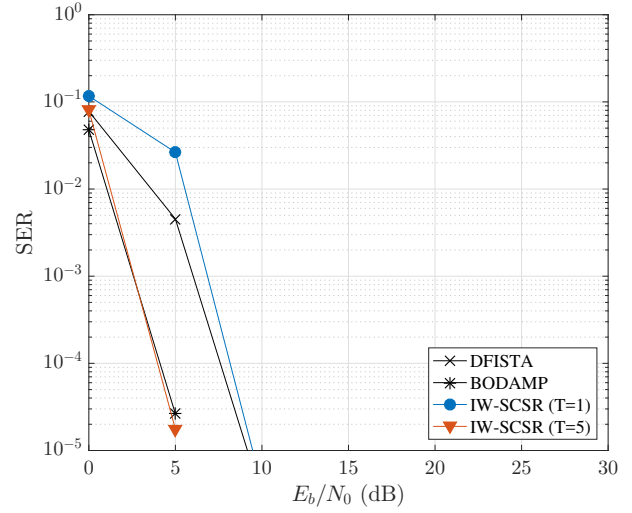


Fig. 6. SER performance ( $M = 60, N = 80, N_o = 10$ )

which is based on FISTA (Fast Iterative Shrinkage Thresholding Algorithm) [11] for compressed sensing, and BODAMP (Bayes Optimized Discreteness-aware AMP)[13], which is based on AMP (Approximate Message Passing) [12] for compressed sensing.

Figures 3–6 show the SER performance for the four different parameter sets  $(M, N, N_o) = (6, 8, 7), (6, 8, 1), (60, 80, 70), (60, 80, 10)$ , respectively. From the performance of DFISTA and BODAMP, we can confirm that the precoding by the DFT matrix implicitly equipped in the SC-CP signaling has comparable capability as the Hadamard matrix considered in [9]. Thus, we are now free from the operations of IDFT and precoding at the IoT transmitter side. Moreover, by comparing the performance of IW-SCSR with  $T = 1$  and 5, we can see that considerable performance gain is achieved by  $T = 5$ , which justifies the validity of update equations of (17) and

(18). Note that, as the number of zero symbols increases, IW-SCSR achieves better performance compared to DFISTA owing to the employment of the sparse regularizer. Also, IW-SCSR with  $T = 5$  outperform other methods for all parameter sets, while the performance of BODAMP is equivalent to that of IW-SCSR with  $T = 5$  for  $(M, N, N_o) = (60, 80, 10)$ . It should be noted that it may be possible to further improve the performance of IW-SCSR by more appropriate choice of  $\beta, \rho, T$  in our future work.

## VI. CONCLUSION

We have proposed overloaded SC-CP signal detection scheme for uplink IoT environments via IW-SCSR optimization approach. Unlike the OFDM based approach in [9], the proposed scheme require neither IDFT operation nor precoding matrix multiplication at the transmitter side, the proposed

approach is suited to the IoT data collection scenario, where cost, capability and energy of the transmitter are extremely limited. The validity of the proposed approach using SC-CP signaling and IW-SCSR optimization is confirmed via computer simulations

Future work includes the investigations of more appropriate system parameters and more sophisticated detection algorithm taking advantage of group sparsity in the block transmission schemes.

#### REFERENCES

- [1] A. Gupta and R. K. Jha, "A survey of 5G network: Architecture and emerging technologies," *IEEE Access*, vol. 3, pp. 1206–1232, July 2015.
- [2] J. G. Andrews, S. Buzzi, W. Choi, S. V. Hanly, A. Lozano, A. C. Soong, and J. C. Zhang, "What will 5G be?," *IEEE Journal on Selected Areas in Communications*, vol. 32, no. 6, pp. 1065–1082, June 2014.
- [3] A. K. Saxena, I. Fijalkow, A. L. Swindlehurst, "Analysis of one-bit quantized precoding for the multiuser massive MIMO downlink," *IEEE Trans. on Signal Process.*, vol. 65, no. 17, pp.4624–4634, Sep. 2017.
- [4] S. Jacobsson, G. Durisi, M. Coldrey, C. Studer, "Massive MU-MIMO-OFDM downlink with one-bit DACs and linear precoding," 2017. [Online]. Available: <http://arxiv.org/abs/1704.04607>
- [5] Y. Nin, H. Matsuoka, Y. Sanada, "Performance comparison of overloaded MIMO system with and without antenna selection," *IEICE Trans. Commun.*, vol. E100-B, no. 5, pp. 762–770, May 2017.
- [6] D. L. Donoho, "Compressed sensing," *IEEE Trans. Inf. Theory*, vol. 52, no. 4, pp. 1289–1306, Apr. 2006.
- [7] K. Hayashi, M. Nagahara, T. Tanaka "A user's guide to compressed sensing for communications systems," *IEICE Trans. Commun.*, vol. E96-B, no. 3, pp. 685–712, Mar. 2013.
- [8] R. Hayakawa, K. Hayashi, "Convex optimization-based signal detection for massive overloaded MIMO systems," *IEEE Trans. Wireless Commun.*, vol. 16, no. 11, pp. 7080–7091, Nov. 2017.
- [9] K. Hayashi, A. Nakai, R. Hayakawa, S. Ha, "Uplink Overloaded MU-MIMO OFDM Signal Detection Methods using Convex Optimization", in *Proc. 2018 APSIPA Annual Summit and Conference (APSIPA ASC 2018)*, Honolulu, Hawaii, USA, pp. 1421-1427, Nov. 2018.
- [10] R. Hayakawa and K. Hayashi, "Reconstruction of complex discrete-valued vector via convex optimization with sparse regularizers," *IEEE Access*, vol. 6, pp. 66 499–66 512, Dec. 2018.
- [11] A. Beck and M. Teboulle, "A fast iterative shrinkage-thresholding algorithm for linear inverse problems," *SIAM J. Imag. Sci.*, vol. 2, no. 1, pp. 183–202, Mar. 2009.
- [12] D. L. Donoho, A. Maleki, and A. Montanari, "Message-passing algorithms for compressed sensing," *Proc. Nat. Acad. Sci.*, vol. 106, no. 45, pp. 18914–18919, Nov. 2009.
- [13] R. Hayakawa and K. Hayashi, "Discreteness-aware approximate message passing for discrete-valued vector reconstruction," *IEEE Trans. Signal Process.*, vol. 66, no. 24, pp. 6443–6457, Dec. 2018.